Journal of Laser Applications

Real-time prediction of quality characteristics in laser beam welding using optical coherence tomography and machine learning

Cite as: J. Laser Appl. **32**, 022046 (2020); https://doi.org/10.2351/7.0000077
Submitted: 01 April 2020 • Accepted: 01 April 2020 • Published Online: 05 May 2020

Christian Stadter, Maximilian Schmoeller, Lara von Rhein, et al.

Journal of Laser Applications ARTICLE scitation.org/journal/jla

Real-time prediction of quality characteristics in laser beam welding using optical coherence tomography and machine learning

Cite as: J. Laser Appl. 32, 022046 (2020); doi: 10.2351/7.0000077
Submitted: 1 April 2020 · Accepted: 1 April 2020 ·
Published Online: 5 May 2020

Christian Stadter, Maximilian Schmoeller, Lara von Rhein, and Michael F. Zaeh

AFFILIATIONS

Institute for Machine Tools and Industrial Management (iwb), Technical University of Munich, Boltzmannstrasse 15, 85748 Garching, Germany

Note: This paper is part of the Special Collection: Proceedings of the International Congress of Applications of Lasers & Electro-Optics (ICALEO® 2019).

ABSTRACT

Laser beam welding significantly outperforms conventional joining techniques in terms of flexibility and productivity. The process benefits, in particular, from the highly focused energy and thus from a well-defined heat input. The high intensities of brilliant laser radiation, however, induce very dynamic effects and complex processes within the interaction zone. The high process dynamics require a consistent and reliable quality assurance to ensure the required weld quality. A novel sensor concept for laser material processing based on optical coherence tomography (OCT) was used to measure the capillary depth of the keyhole during deep penetration welding. The OCT measurements were compared with analyses of the surface quality of the weld seams. A machine learning approach could be utilized to reveal correlations between the weld depth signal and the weld seam surface quality, underlining the high level of information contained in the OCT signal about characteristic process phenomena that affect the weld seam quality. Fundamental investigations on aluminum, copper, and galvanized steel were carried out to analyze the structure of the data recorded by the OCT sensor. Based on that, evaluation strategies focusing on quality characteristics were developed and validated to enable a valid interpretation of the OCT signal. The topography of the weld seams was used to classify the surface quality and correlated with the weld depth signal of the OCT system. For this purpose, a preprocessing of the OCT data and a detailed analysis of the topographic information were developed. The processed data were correlated using artificial neural networks. It was shown that by using adequate network structures and training methods, the inline process data of the capillary depth can be used to predict the surface quality with decent prediction accuracy.

Key words: predictive quality, machine learning, artificial neural networks, process data, data interpretation

I. INTRODUCTION

One major challenge in the large-scale industrial application of laser beam welding is the comprehensive assurance of the weld seam quality. Real-time process monitoring to ensure continuous traceability and a holistic quality assurance is an essential requirement for more and more applications. Due to the high process dynamics and the intense process emissions, laser beam welding places particularly high demands on observation systems. Conventional methods are either based on the evaluation of indirect process quantities, such as secondary process emissions, or require costly offline inspection steps. The measurement methods used so far for inline purposes provide very limited information about the process phenomena and the resulting weld seam properties.

To exploit the advantages of flexible and productive laser-based manufacturing processes, an inline process monitoring system is indispensable. Optical coherence tomography (OCT) enables a direct measurement of the topology within the process zone in real time, independent of process emissions and metal vapor or plasma. Special challenges arise in evaluating the temporally high-resolution data, which are superimposed with the complex and dynamic phenomena in the process zone to draw reliable conclusions about the weld seam quality. Machine learning

provides a powerful tool for evaluating the capillary depth data recorded *in situ* during laser beam welding and interpreting these data with regard to the resulting seam properties.

II. OPTICAL COHERENCE TOMOGRAPHY

Based on the principle of low coherence interferometry and the optical interferometer design proposed by Michelson, OCT has been established as a method for performing high-precision distance measurements since 1972. A broadband light source rather than a narrow-band laser beam source allows the absolute distance to be evaluated from the interference pattern.[1] The development of a lateral scanning device enabled topographic images to be taken of the eye from 1991 onward. The capability of the method and the subsequent establishment of OCT in ophthalmology are based on showing that a fraction as small as 10^{-10} times the incident optical power reflected at the sample is sufficient for robust distance measurement.[2] Further research has focused on evaluating the interference in the frequency domain (FD) rather than in the time domain (TD).[3] Thus, the acquisition time for topographic scans could be reduced drastically. Likewise, it could be shown that the sensitivity of the FD is superior to that of the TD OCT.[4] This made high-precision measurements[5] with a temporal resolution of several kilohertzs possible.[6]

Figure 1 shows the optical concept of FD OCT. Characteristic is the fixed reference path free of moving parts. Since no adjustment of the mirror is necessary, the acquisition rate is only limited by the sampling rate of the detector array. The spectral analysis of the interference between the reference and the measuring beam is performed by means of a spectrometer.

Based on the polychromatic illumination with the complex electric field,

$$E_i = s(k, \omega)e^{i(kz-\omega t)} \tag{1}$$

and assuming a wavelength independent splitting ratio of the beam splitter of 0.5, the electric fields in the reference and the measurement path (cf. Fig. 1) can be determined as[8]

$$E_R = \frac{E_i}{\sqrt{2}} r_R e^{i2kz_R}, \quad E_S = \frac{E_i}{\sqrt{2}} \sum_{n=1}^{N} r_{Sn} e^{i2kz_{Sn}}. \tag{2}$$

Here, s is the amplitude of the electric field depending on the wave number k and the angular frequency ω, z is the coordinate in beam propagation direction, and t is the time. For the general case of transparent media, multiple reflections n at the position z_{Sn} and the respective power reflectivity $R_{Sn} = |r_{Sn}|^2$ are considered. The photocurrent in the detector I_D results from the superposition of the electric fields from the reference and measurement path,[8]

$$I_D(k, \omega) = \frac{\rho}{2} \langle |E_R + E_S| \rangle^2, \tag{3}$$

where ρ describes the responsivity of the sensor and $\langle \cdot \rangle$ is the time average, i.e., the integration over the response time of the detector,[6]

$$\langle f \rangle = \lim_{T \to \infty} \frac{1}{2T} \int_{-T}^{T} f(t) dt, \tag{4}$$

with Eqs. (1) and (2), the temporally invariant terms of the detector current can be quantified,[8]

$$\begin{aligned} I_D(k) = & \frac{\rho}{4}[S(k)(R_R + R_{S1} + R_{S2} + \cdots)] \\ & + \frac{\rho}{4}\left[S(k) \sum_{n=1}^{N} \sqrt{R_R R_{Sn}} (e^{i2k(z_R - z_{Sn})} + e^{-i2k(z_R - z_{Sn})})\right] \\ & + \frac{\rho}{4}\left[S(k) \sum_{n \neq m=1}^{N} \sqrt{R_{Sn} R_{Sm}} (e^{i2k(z_{Sn} - z_{Sm})} + e^{-i2k(z_{Sn} - z_{Sm})})\right]. \end{aligned} \tag{5}$$

The spectral power as a function of wave number $S(k)$ can be simplified with regard to the light sources typically used for FD OCT. Assuming a Gaussian shaped spectrum, the spectral power becomes[8]

$$S(k) = \langle |s(k, \omega)|^2 \rangle = \frac{1}{\Delta k \sqrt{\pi}} e^{-\left[\frac{k-k_0}{\Delta k}\right]^2}. \tag{6}$$

Here, k is the central wave number and Δk is the spectral bandwidth of the light source spectrum. To obtain the distance z_S, $\sqrt{R_S(z_S)}$ can be specified for the case of discrete reflections N as the sum $\sum_{n=1}^{N} \sqrt{R_{Sn}} \delta(z_S - z_{Sn})$.

Inverse Fourier transformation of Eq. (4) reveals the information about the axial position of the reflection planes. Figure 2 illustrates an exemplary detector signal in FD OCT and the corresponding signal after Fourier transformation considering two reflections in the measurement path. A detailed mathematical deduction of suitable simplifications taking into account the measuring principle can be found in Ref. 8.

An in-depth discussion of measurement parameters important for practical applications depending on the spectral characteristics of the setup is given in Ref. 9.

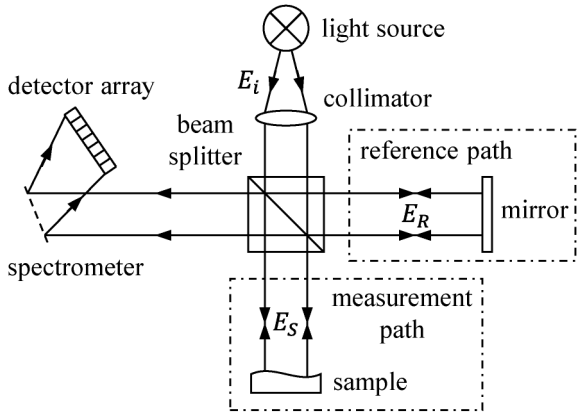

FIG. 1. Optical concept of Fourier domain OCT (based on Ref. 7).

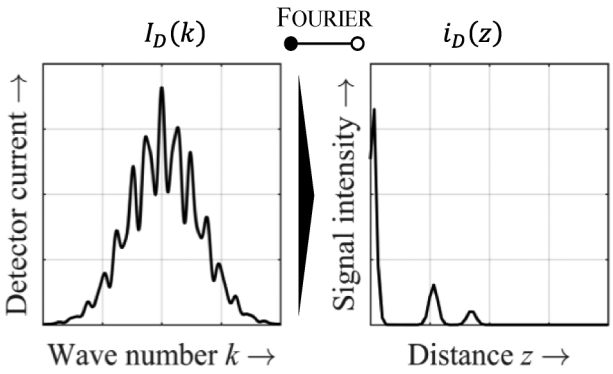

FIG. 2. Raw detector signal as a function of the wave number (left) and Fourier transformed signal (right) in FD OCT (based on Ref. 7).

III. STATE OF THE ART

A. Inline quality assurance in laser beam welding

For the monitoring of laser material machining processes, mainly optical methods have been established.[10] Particularly for laser beam welding, the properties of the noncontact measuring principle and the high accuracy of optical systems have proven to be advantageous for monitoring and controlling purposes.[11]

De Bono *et al.* investigated optical sensor approaches for real-time monitoring of laser beam welding processes. Photodiodes monitoring between 600 and 850 nm were used to measure the process emissions in butt welding and stake welding trials. Based on welds with reference conditions, further welds with known defects were performed and then analyzed by means of the captured photodiode signals. Process anomalies due to an incorrect beam power, a joint contamination, and a joint gap could be detected. Also, optical coherence tomography has been employed to coaxially measure the capillary depth using a fixed optics setup. It could be proven that the system can monitor the capillary depth during partial penetration welding.[12]

Kogel-Hollacher *et al.* discussed the capability of chromatic coded and low coherence interferometry sensors for ultrafast and inline measurements in micro- and macro-laser processing. A chromatic line sensor could be utilized to measure the topography of surfaces with up to 400 000 points per second. Even under challenging conditions, such as polished, sloped surfaces, a resolution in the sub-micrometer range could be achieved. Moreover, surface profiles were taken using optical coherence tomography. A scanner device was used to deflect the measuring and the processing laser beam coaxially. The setup enabled *in situ* recordings of the surface topography during surface processing with ultrashort laser pulses.[13]

Webster *et al.* developed a system based on optical coherence tomography for remote processing. Applying the measuring beam coaxially to the processing beam allowed the depth in remote machining to be monitored. Based on the measurements, an automatic sculpting of 3D structures could be demonstrated.[14] Aiming at an automated laser machining, the approach has been further developed by means of a closed-loop feedback control. The system allowed for resolving the machining depth with up to 230 kHz and an axial resolution of about 7 μm.[15]

Schmoeller *et al.* investigated the inline-measurement of the weld depth for high-brilliance laser radiation using optical coherence tomography. The influence of the material, the weld depth, and the angle of incidence of the processing beam on the capillary depth signal were assessed for both multimode and singlemode laser radiation. The effect of the three influencing factors was quantified by statistical measures. The work could demonstrate the applicability of OCT for weld depth measurements with singlemode radiation and spot sizes down to 55 μm.[16]

Further studies in the preprocess and postprocess zones have shown the possibilities of process control with regard to adapting the seam position and quality assurance. By investigating fundamental influencing factors on the OCT measurement, it was possible to quantify the accuracy as a function of the material, the angle of incidence, and process-related interferences.[17]

B. Data classification using artificial neural networks

Artificial neural networks have proven to be a simple and effective tool for feature detection, especially when the detection of correlations is difficult to express by explicit rules. This machine learning method is not only of central importance in the field of computer science but also an essential component in the continuous development of laser machining applications. Therefore, the following review will focus on applications of neural networks as the most popular self-learning tool[18] for quality prediction in laser machining.

Mayr *et al.* evaluated different machine learning approaches for quality monitoring during laser welding of hairpins; 500 laser welded hairpin contacts have been analyzed and used as a database for the prediction of the weld quality. The copper welds were evaluated offline by means of a CCD camera capturing polychrome images from three perspectives and resistance as well as weight measurements. Five weld defects have been considered, with each sample being assigned a defect severity between zero and three. Four different machine learning algorithms were implemented to predict the weld quality based on the machine parameters. Applying a binomial classification that accounts for the occurrence and not for the severity of the defects, prediction scores of approx. 90% (F1 score) were achieved.[19]

Yu *et al.* developed a quality assurance system for laser welding of aluminum. Three photodiode sensors were attached at different angles to the welding optics to measure the process emissions generated by plasma with a sampling rate of 10 kHz. The laser power and the wire feed rate were configured to induce plasma emissions of varying intensity. Tensile tests were taken to assess the mechanical strength of the welds. To predict the weld quality, two procedures were followed in parallel: an artificial neural network was implemented to predict the tensile strength based on the measured signals. Besides that, a fuzzy multifeature pattern recognition algorithm was deployed to classify the weld quality. The data preprocessing was based on a temporal averaging of the recorded signal curves.[20]

You *et al.* utilized a multiple optics sensing system for process monitoring and defect diagnosis in laser welding. The signals from

photodiode sensors and a spectrometer were analyzed by means of a wavelet packet decomposition principal component analysis (WPD-PCA) to extract welding features. An image processing approach including visual, auxiliary illumination, and x-ray systems was chosen to determine the welding status. Machine learning algorithms then allowed for the development of correlation models that revealed the relationship between optical features and geometrical parameters as well as between optical features and welding defects.[21]

Knaak *et al.* presented an approach to assess high-dimensional sensor data such as camera-based process recordings or multiple-sensor datasets. Images from two types of sensors were first transformed by a principal component analysis and then classified according to the weld quality. It could be shown that the principal component analysis allowed for a significant reduction of the dimensionality with hardly any loss of information. Four classes with respect to the considered weld seam imperfections were attributed and tested by the implemented algorithms. Special attention was paid to identify relevant features to detect the defined categories of the seam quality. When choosing the right features, it could be shown that the defined welding defects can be detected with an accuracy of 99.9%, demonstrating the possibilities of an efficient and reliable analysis of high-dimensional sensor data.[22]

IV. OBJECTIVES AND APPROACH

Process monitoring of laser beam welding has been the focus of intensive research for a long time due to the inherent challenges of the process. Optical coherence tomography has proven to be a powerful tool for gathering direct process information despite the intense emissions during welding that often induce interpretation errors when using other technologies. However, in order to assess the process data in real-time and to use it for a robust quality assurance, a suitable evaluation methodology is required. Fundamental investigations were thus carried out for the automated evaluation of the OCT data, on the basis of which a quality statement is possible during the runtime of the welding process. A methodology was established to preprocess the data, train an artificial neural network and predict the weld seam quality, cf. Fig. 3. Based on the surface quality of the weld seam, an evaluation of the seam quality was developed in order to demonstrate the derivation of quality parameters from the inline recorded data.

V. EXPERIMENTAL SETUP

The welding experiments were performed using a robot-based fixed optics system. The welding optics of the type Precitec YW52 was equipped with the FD OCT system Precitec IDM. The optical setup of the welding optics and the integrated measuring system are shown in Fig. 4. IPG's YLR-8000 emitting at 1070 nm delivered the multimode laser radiation of up to 8 kW. A fiber core diameter of 200 μm and an image ratio of 1:1.6 resulted in a spot size of about 320 µm. Additionally, a singlemode laser beam source IPG YLR-3000-SM with a maximum output power of 3 kW provided high-brilliance radiation.

A fiber core diameter of 30 μm allowed for spot sizes of about 55 μm. The OCT system measured at 1550 ± 20 nm with an acquisition rate of 70 kHz and an optical power of 10 mW. The size of the measuring spot in the focal plane was about 50 μm in diameter. The measuring beam passes through the same optical path as the processing beam, which enables coaxial process observation. The measuring light emitted by a superluminescent diode was divided by a beam splitter module into a keyhole and a surface measuring beam.

Between 55% and 100% of the measuring light could be directed into the capillary. The intensity required to measure the surface topology strongly depends on the material properties and was set such that as much measuring power as possible could be used for the depth measurement. By utilizing the beam splitter module, the capillary depth could be determined directly by the difference between surface and depth signal.

With regard to the challenges concerning process control in copper welding, which requires precise quality assurance, the oxygen-free copper alloy C10200 (sheet thickness 3 mm) was chosen. The topographic measurements of the OCT system were validated with a Keyence VR 3100 3D macroscope equipped with both micro- and macro-cameras.

With regard to the universal data evaluation approach, a wide range of parameter combinations was examined. Both multimode

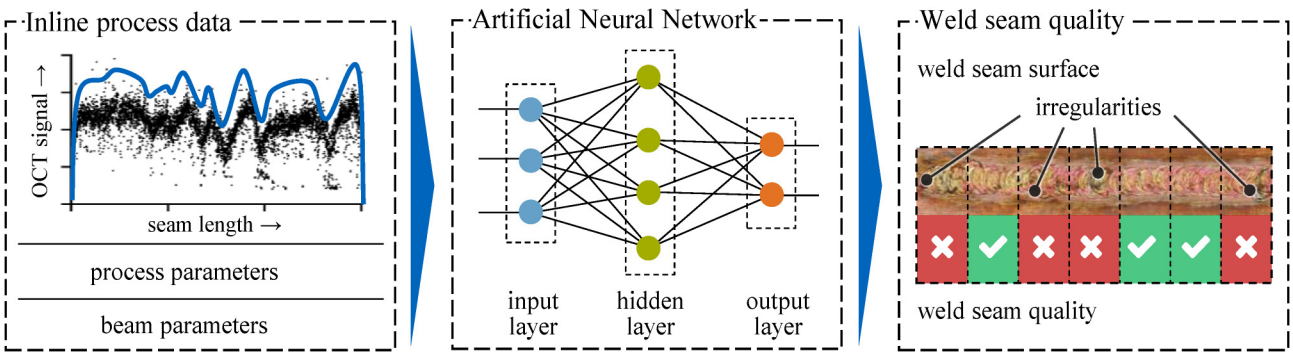

FIG. 3. Prediction of the weld seam quality based on the inline recorded process data by OCT and artificial neural networks.

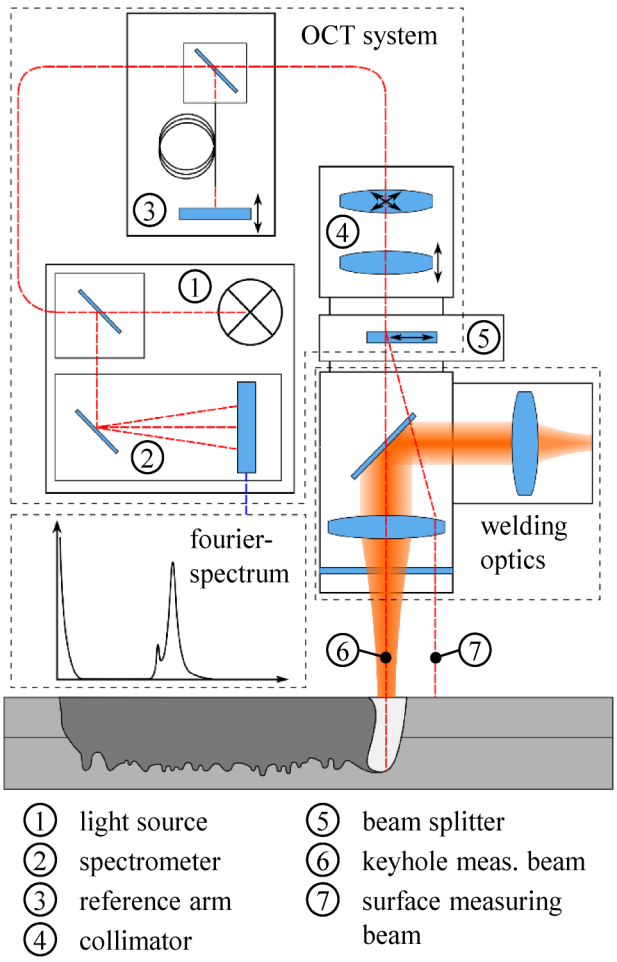

FIG. 4. Optical setup of the welding optics equipped with the sensor system based on FD OCT.

as well as singlemode radiation with power levels between 3 and 6 kW and angles of incidence between −20 and +20° were applied. The parameter levels considered in the experiments can be found in Table I. A total of 58 welding trials were considered for the data evaluation process and the prediction of the weld quality.

TABLE I. Welding parameters and considered values.

Parameter	Investigated values
Laser power	[3, 6] kW
Welding speed	[5, 7.5, 10] m/min
Angle of incidence	[−20, −15, −10, 10, 15, 20]°
Radiation mode	[singlemode, multimode]

VI. ANALYSIS OF THE WELD SEAM SURFACE

The artificial neural network employed to predict the weld seam quality requires labeled training datasets. For the supervised training of the neural network, an evaluation of the seam quality is therefore necessary. The weld quality was evaluated on the basis of the height profile along the weld center. A discrete wavelet analysis of the height profile was performed in order to quantify the characteristics of the weld seam surface and make them available for the training of the neural network. The wavelet transformation allows many classes of natural signals to be processed computationally efficiently with the intention of image compression, noise reduction or pattern recognition.[23] Due to the possibility of extracting signal characteristics, a discrete wavelet decomposition was used to develop an objective criterion for assessing surface quality.

Similar to the Fourier analysis, wavelet analysis is based on the division of the basis function into shifted and scaled components. The basis function meets the following two basic conditions:[24]

$$\int_{-\infty}^{\infty} \psi(t)\, dt = 0, \qquad \int_{-\infty}^{\infty} |\psi(t)|^2 dt < \infty. \tag{7}$$

A common and simple orthonormal function that meets these requirements is the Haar wavelet,[24]

$$\psi = \begin{cases} 1 & 0 \le t < 1/2, \\ -1 & 1/2 \le t < 1, \\ 0 & \text{otherwise.} \end{cases} \tag{8}$$

The wavelet analysis represents the original signal by approximations a_i and details d_i. The original signal is first decomposed by a level 1 approximation and a level 1 detail. Then, the level 1 approximation is again broken down into a level 2 approximation and a level 2 detail and so on.

Since preliminary investigations showed that an analysis at level 5 revealed the best correlations to defects in the weld surface, a decomposition of the original height profile s at level 5 was performed,

$$s = a_5 + d_5 + d_4 + d_3 + d_2 + d_1. \tag{9}$$

An exemplary height profile and the corresponding wavelet decomposition at level 5 can be seen in Fig. 5.

The best correlations to weld defects were identified by analysis of details d_2. It was found that characteristics of the weld surface indicative of weld defects are reflected in fluctuations in signal d_2. Therefore, the height and the frequency of bursts in signal d_2 were evaluated and used for the quality assessment. Peaks with a minimum step height of 0.02 mm were considered significant and counted within the examined weld section (cf. Fig. 5).

To evaluate the quality of the welds, sections of about 5 mm were considered. The length of the sections was chosen so that a visual inspection could be carried out and the evaluation of the wavelet analysis could be validated. One section contained 2500 measuring points, which corresponds to a length of 4.5 mm with an acquisition rate of 70 kHz and a welding speed of 7.5 m/min.

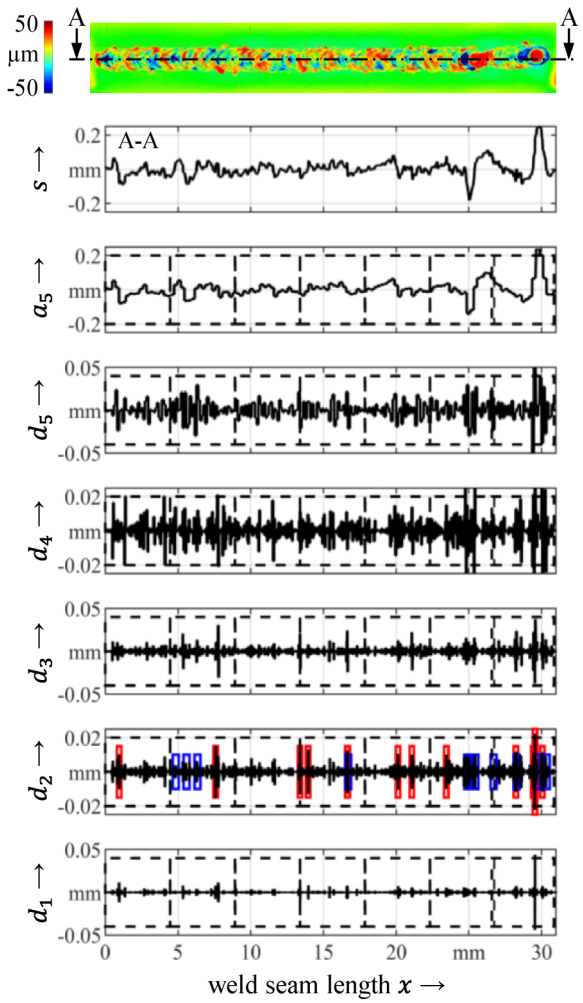

FIG. 5. Wavelet analysis at level 5 of the height profile along the weld center.

Weld seam sections, in which more than seven peaks were counted in signal d_2, were classified as poor and with fewer irregularities as good. The classification was then validated by a visual inspection to verify the choice of parameters for peak detection.

In this section, the evaluation of the weld quality on the basis of the height profile will be discussed in more detail. Specifically, the weld quality in the respective section is considered to be poor if the following objective criteria are assigned to signal d_2:

- The number of large individual peaks n_{ind} exceeds eight within a section. Peaks >0.02 mm are counted once, and peaks >0.04 mm are counted twice.
- The number of medium peaks n_{adj} adjacent to each other exceeds seven. In accordance with visual inspections, peaks >0.005 mm were classified as medium-high.

These criteria were determined on the basis of preliminary studies, the aim of which was to reproduce the quality assessment by means of visual inspections. The application of these criteria to the weld profile of a typical copper weld and the prediction of the weld seam quality are shown in Fig. 6.

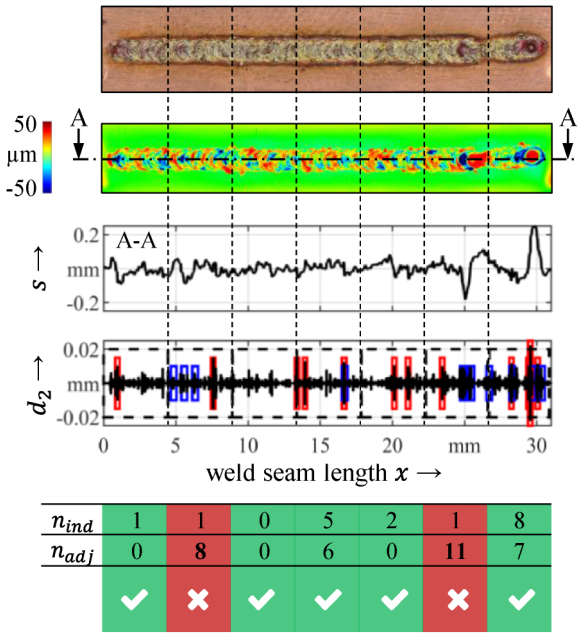

FIG. 6. Quality criteria to classify the weld seam based on the height profile.

Although the limit values were determined in advance on the basis of visual inspections of the weld surface and subsequently validated on selected samples, there is still the greatest potential for optimizing the methodology presented in this work.

VII. PREPROCESSING OF THE INLINE OCT DATA

The preprocessing of the input data has a decisive influence on the prediction accuracy and the generalizability of the results of the neural network. As a matter of principle, a trade-off has to be found. Basically, a certain minimum of data is necessary to allow the network to use sufficient process information to recognize patterns for a correlation with the weld quality. Also, the considered weld seam sections should be selected to ensure a large enough segment to permit a visual inspection to check the classification of the weld quality. On the other hand, a high degree of complexity regarding the network structure and training is required to process large amounts of input data. As the number of neurons increases, so does the risk of overfitting and limited generalizability of the network. The number of sections available for training also decreases with increasing section length. This means that fewer samples are available for training the algorithm, which can significantly reduce the prediction quality.

The selected section length of about 4.5 mm, therefore, represents a result of the listed requirements. Since the number of measured capillary depth values within a section is 2500, a suitable preprocessing of the OCT data is necessary. Figure 7 shows the raw signal recorded during a coaxial depth measurement using OCT.

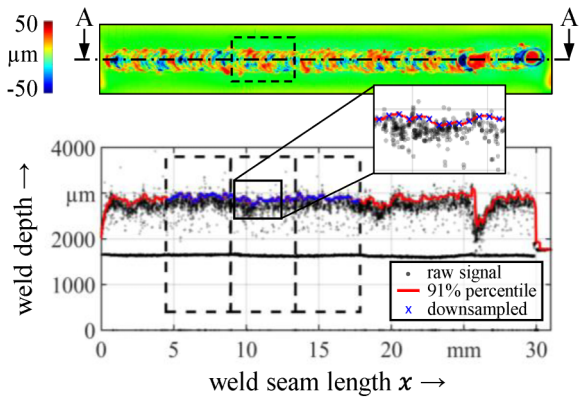

FIG. 7. Filtering and downsampling of the OCT data applied to a section of the weld seam and associated weld seam topography.

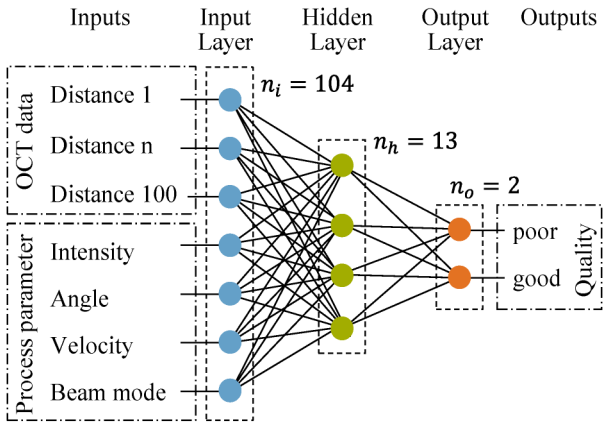

FIG. 8. Input/output parameters and the architecture of the neural network used to predict the weld quality.

Due to the high process dynamics of deep penetration welding, the signal is scattered in depth direction. From the raw signal, the 91% percentile was calculated over a window width of 255 samples in order to smooth the curve.

In the second step, the range, for which the OCT data were evaluated, was extended relative to the weld section under consideration for the seam quality analysis. Figure 7 (top) shows an example of the weld area for which the seam quality was to be predicted. The OCT data were also evaluated for the leading and the trailing weld section, since investigations have shown that this data basis is the best for identifying correlations to the weld quality. Lastly, the percentile filtered data were downsampled in time. A lowpass Chebyshev Type I infinite impulse response filter of order 8 was applied to reduce the total number of data points from 7500 to 100. The reduction of the process data has the advantage that a varying number of measuring points due to a changing welding speed at a constant acquisition rate has no significant influence on the data structure or the processing.

VIII. PREDICTION OF THE WELD SEAM QUALITY BASED ON MACHINE LEARNING

For predicting the weld seam quality, a feedforward pattern recognition neural network was designed. The basic architecture is illustrated in Fig. 8. The preprocessed OCT data as well as the process parameters were used as input. Of relevance are the intensity, the angle of incidence of the laser beam, the welding speed, and the radiation mode. With the preprocessed OCT data, a total of 104 input neurons were generated. Two output neurons represent the binomial classification of the weld seam quality. The division of the weld seams into finite sections resulted in a total of 549 sections, which, together with the captured OCT data, were available as test samples for predicting the weld quality.

In a preliminary study, three methods for training the network were examined

- Scaled conjugate gradient backpropagation;
- Levenberg–Marquardt backpropagation; and
- Bayesian regularization backpropagation.

Training experiments with a varying number of neurons were carried out and evaluated on the basis of the performance and the quota of correctly assigned samples as well as the variance of the results. The best results were obtained using the Levenberg–Marquardt backpropagation algorithm. Applying the scaled conjugant gradient backpropagation method, a significantly higher scatter of the performance values was observed. The ratio of the correctly assigned samples was also slightly below that of the Levenberg–Marquardt algorithm. Significantly higher performance values and correct allocations close to 100% were achieved with Bayesian regularization backpropagation. Although the algorithm provides good generalization properties,[25] it was not used due to a strong tendency to overfitting that has been observed on the training data for a wide range of network parameters.

To design the network architecture, the number of neurons in the hidden layer was systematically varied. Neuron numbers between 5 and 100 were investigated. With an increasing number of neurons, a slightly improved performance can be observed. At the same time, the variance of the performance and the prediction accuracy increased slightly, see Fig. 9. The performance criterion used was the mean squared error.

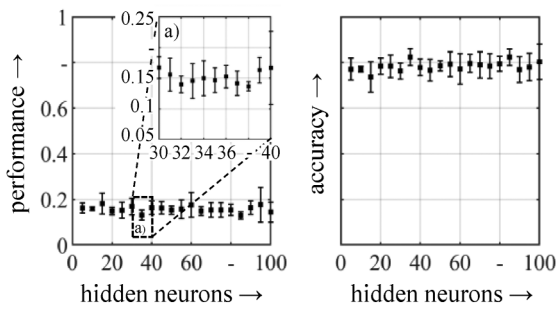

FIG. 9. Performance and accuracy of the neural network depending on the number of hidden neurons.

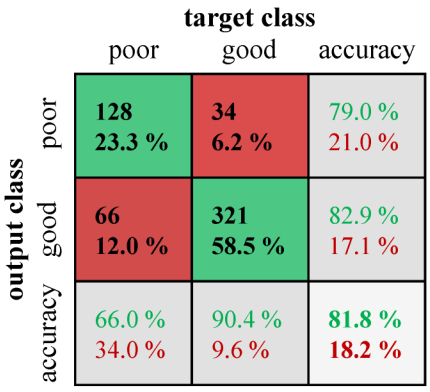

FIG. 10. Confusion matrix for a neural network with 36 hidden neurons, showing the false positive (type I error, 6.2%) and the false negative (type II error, 12.0%) of the weld quality prediction

The lowest variance and the highest prediction accuracy were achieved with 36 neurons in the hidden layer. The slight increase in variance is accompanied by a tendency to overfitting, which was observed at high neuron numbers. While the prediction accuracy on the training data rose with an increasing number of neurons, the score on the test data decreased. Although a similar performance was achieved in the range of 85 neurons, the neuron number of 36 was chosen as optimal to counteract the tendency to overfitting and to ensure transferability to new datasets. For this reason, 15% of the data were used for validation rather than the usual 10%,[26] 15% for testing, and 70% for training the network.

The prediction accuracy of a neural network consisting of 36 neurons in the hidden layer can be seen by the error matrix plotted in Fig. 10. Of the 162 samples for which poor quality was predicted, 128, or 79%, were actually in this class. Of the well predicted weld sections, 82.9% were correctly assigned. A total of 81.8% of the weld sections were correctly predicted.

For the trained neural network, the time required to process the input data to predict the weld quality was 385 ms for all 549 samples (CPU: i7-6700HQ, 4 Processors, 2.60 GHz; RAM: 16 GB). With a processing time of roughly 700 μs per weld section, the network's advantage in predicting the process data for a wide range of process parameters and for both multimode and singlemode radiation with decent accuracy becomes clear.

IX. CONCLUSIONS AND OUTLOOK

After developing a method to predict quality characteristics based on inline process data captured by OCT, the following insights can be concluded:

- Discrete wavelet transformation can be used to fundamentally classify the weld quality based on the height profile.
- A lowpass Chebyshev Type I infinite impulse response filter allows us to drastically reduce the amount of process data without significantly affecting the informational content.
- Machine learning allows an implicit use of the information contained in the OCT signal regarding process-determining effects and phenomena for the prediction of quality characteristics.
- Artificial neural networks provide a real-time analysis of the *in situ* process data for a broad range of process regimes.

The work shows that the process data recorded for the welding depth can be correlated with the quality of the weld seam surface and thus illustrates the considerable information content of the OCT data. Further research will focus on the classification of the weld seam quality based on objective criteria, which ultimately have a decisive influence on the prediction accuracy. Also, the optimization of the architecture of the machine learning algorithms will be addressed in detail.

ACKNOWLEDGMENTS

The results presented were achieved within the RoKtoLas project, which is supported by the German Federal Ministry of Education and Research (BMBF) within the Photonics Research Germany funding program (Contract No. 13N14555) and supervised by the VDI Technology Center (VDI TZ). The authors would like to acknowledge the BMBF and the VDI TZ for their support and for the effective and trusting cooperation.

REFERENCES

[1]P. A. Flournoy, R. W. McClure, and G. Wyntjes, "White-light interferometric thickness gauge," Appl. Opt. **11**, 1907–1915 (1972).
[2]D. Huang, E. Swanson, C. Lin, J. Schuman, W. Stinson, W. Chang, M. Hee, T. Flotte, K. Gregory, C. Puliafito *et al.*, "Optical coherence tomography," Science **254**, 1178–1181 (1991).
[3]S. R. Chinn, E. A. Swanson, and J. G. Fujimoto, "Optical coherence tomography using a frequency-tunable optical source," Opt. Lett. **22**, 340–342 (1997).
[4]J. F. de Boer, B. Cense, B. H. Park, M. C. Pierce, G. J. Tearney, and B. E. Bouma, "Improved signal-to-noise ratio in spectral-domain compared with time-domain optical coherence tomography," Opt. Lett. **28**, 2067–2069 (2003).
[5]J. M. Fraser, "Laser process monitoring and automatic control at kHz rates through inline coherent imaging," AIP Conf. Proc. **1464**, 492–496 (2012).
[6]R. Bernardes and J. Cunha-Vaz, *Optical Coherence Tomography*, Biological and Medical Physics, Biomedical Engineering (Springer, Heidelberg, 2012).
[7]A. Donges and R. Noll, *Laser Measurement Technology*, Springer Series in Optical Sciences 188 (Springer, Heidelberg, 2015).
[8]W. Drexler, *Optical Coherence Tomography*, Biological and Medical Physics, Biomedical Engineering (Springer, Berlin, 2008).
[9]P. H. Tomlins and R. K. Wang, "Theory, developments and applications of optical coherence tomography," J. Phys. D Appl. Phys. **38**, 2519–2535 (2005).
[10]T. Purtonen, A. Kalliosaari, and A. Salminen, "Monitoring and adaptive control of laser processes," Phys. Proc. **56**, 1218–1231 (2014).
[11]S. K. Lee and S. J. Na, "A study on automatic seam tracking in pulsed laser edge welding by using a vision sensor without an auxiliary light source," J. Manuf. Syst. **21**, 302–315 (2002).
[12]P. de Bono, C. Allen, G. D'Angelo, and A. Cisi, "Investigation of optical sensor approaches for real-time monitoring during fibre laser welding," J. Laser Appl. **29**, 022417 (2017).
[13]M. Kogel-Hollacher, M. Schoenleber, J. Schulze, J. F. Pichot *et al.*, "Inline measurement for quality control from macro to micro laser applications," SPIE Proc. **10091**, 100910H (2017).
[14]P. J. Webster, L. G. Wright, Y. Ji, C. M. Galbraith, A. W. Kinross, C. van Vlack, and J. M. Fraser, "Automatic laser welding and milling with in situ inline coherent imaging," Opt. Lett. **39**, 6217–6220 (2014).

[15]Y. Ji, A. W. Grindal, P. J. Webster, and J. M. Fraser, "Real-time depth monitoring and control of laser machining through scanning beam delivery system," J. Phys. D Appl. Phys. **48**, 155301 (2015).
[16]M. Schmoeller, C. Stadter, S. Liebl, and M. F. Zaeh, "Inline weld depth measurement for high brilliance laser beam sources using optical coherence tomography," J. Laser Appl. **31**, 022409 (2019).
[17]C. Stadter, M. Schmoeller, M. Zeitler, V. Tueretkan, U. Munzert, and M. F. Zaeh, "Process control and quality assurance in remote laser beam welding by optical coherence tomography," J. Laser Appl. **31**, 022408 (2019).
[18]G. Casalino, "Computational intelligence for smart laser materials processing," Opt. Laser Technol. **100**, 165–175 (2018).
[19]A. Mayr, B. Lutz, M. Weigelt, T. Glabel, D. Kibkalt, M. Masuch, A. Riedel, and J. Franke, "Evaluation of machine learning for quality monitoring of laser welding using the example of the contacting of Hairpin windings," in *Proceedings of the 8th International Electric Drives Production Conference (EDPC), Schweinfurt, Germany, 4–5 December* (IEEE, New York, 2018).
[20]J. Yu, Y. Sohn, Y. W. Park, and J.-S. Kwak, "The development of a quality prediction system for aluminum laser welding to measure plasma intensity using photodiodes," J. Mech. Sci. Technol. **30**, 4697–4704 (2016).
[21]D. You, X. Gao, and S. Katayama, "WPD-PCA-based laser welding process monitoring and defects diagnosis by using FNN and SVM," IEEE Trans. Ind. Electron. **62**, 628–636 (2015).
[22]C. Knaak, U. Thombansen, P. Abels, and M. Kröger, "Machine learning as a comparative tool to determine the relevance of signal features in laser welding," Proc. CIRP **74**, 623–627 (2018).
[23]A. Mertins, *Signaltheorie* (Springer Fachmedien Wiesbaden, Wiesbaden, 2013).
[24]H. Kim and H. Melhem, "Fourier and wavelet analyses for fatigue assessment of concrete beams," Exp. Mech. **43**, 131–140 (2003).
[25]K. K. Aggarwal, Y. Singh, P. Chandra, and M. Puri, "Bayesian regularization in a neural network model to estimate lines of code using function points," J. Comput. Sci. **1**, 505–509 (2005).
[26]K. Backhaus, B. Erichson, R. Weiber *et al.*, "Neuronale Netze," in *Fortgeschrittene Multivariate Analysemethoden*, edited by K. Backhaus (Springer, Berlin, 2015), pp. 295–347

Meet the Authors

Christian Stadter is a research associate and doctoral candidate at the Institute for Machine Tools and Industrial Management (iwb). He studied mechanical engineering at the Technical University of Munich. His current field of research is the application of optical coherence tomography for the laser beam welding of car body components.

Maximilian Schmoeller is a research associate and doctoral candidate at the Institute for Machine Tools and Industrial Management (iwb). He studied mechanical engineering at the Technical University of Munich. His current field of research is the application of optical coherence tomography for the laser beam welding of car body components.

Lara von Rhein studied mechanical engineering at the Technical University of Munich. As part of her final thesis, she researched the analysis of OCT data using artificial intelligence.

Michael F. Zaeh is the head of the Institute for Machine Tools and Industrial Management (iwb) as well as full professor for machine tools and manufacturing technologies at the Technical University of Munich. His research focuses on machine tools, joining and cutting technologies, additive manufacturing technologies, and cognitive systems for machine tools.